Dyes and Pigments 85 (2010) 7–15

Contents lists available at ScienceDirect

Dyes and Pigments

journal homepage: www.elsevier.com/locate/dyepig

Benzodipyrrolenine-based biscyanine dyes: Synthesis, molecular structure and spectroscopic characterization

Oleksiy P. Klochko [a], Iryna A. Fedyunyayeva [a], Sania U. Khabuseva [a], Olga M. Semenova [a], Ewald A. Terpetschnig [b], Leonid D. Patsenker [a,b,*]

[a] SSI "Institute for Single Crystals" of the National Academy of Sciences of Ukraine, 60 Lenin Ave., Kharkov 61001, Ukraine
[b] SETA BioMedicals, LLC, 2014 Silver Court East, Urbana, IL 61802, USA

A R T I C L E I N F O

Article history:
Received 6 May 2009
Received in revised form
17 September 2009
Accepted 24 September 2009
Available online 2 October 2009

Keywords:
Benzodipyrrolenine
Biscyanine dyes
Synthesis
Spectral properties
Fluorescence

A B S T R A C T

A novel method of synthesizing long-wavelength absorbing and emitting bis-trimethine dyes that consists of condensing benzodipyrrolenine dialdehyde with quaternized heterocyclic CH-acidic compounds was used to prepare a series of biscyanines. The new method is more convenient than its conventional counterepart, which relies upon condensation of a quaternized benzodipyrrolenine with Fisher's aldehyde, for the synthesis of a symmetrically substituted dyes that contain various heterocyclic end-groups. Investigations of the spectral and luminescent properties of the dyes in solution revealed that the absorption (596–717 nm) and emission (629–773 nm) maxima of the biscyanines were red-shifted by ~100 nm compared to the parent "monomeric" cyanine that contained only one chromophoric polymethine system. The prepared dyes have high extinction coefficients ($\leq$251,000 M^{-1} cm^{-1}) and quantum yield ($\leq$28%). Substitution of both terminal benzoxazole moieties with indolenine, benzothiazole, 2- and 4-quinoline imparted a red-shift in the absorption and emission maxima but lowered quantum yield.

1. Introduction

Cyanine dyes enjoy widespread use as fluorescent probes and labels in biomedical assay [1–4], sensitive materials for optical storage devices [5,6], photorefractive materials [7], spectral sensitizers for silver halide photography and other inorganic, large band-gap, semiconductor materials [8,9], passive photo-shutters and laser dyes [10,11]. For most of these applications, long-wavelength absorbing dyes having high extinction coefficients and high fluorescence quantum yields are required. One of the conventional methods used to achieve these spectral characteristics consists of preparing the so-called biscyanine dyes, which are molecules comprising two polymethine-type chromophoric systems.

Biscyanine molecules are of significant theoretical interest as the model bifluorophoric system permits investigation of the correlation between the mutual orientation of two polymethine chromophores and their spectral properties such as the shape of absorption and emission spectra, the number and relative intensity of the absorption bands, electron transition energy, extinction coefficient and quantum yield. These investigations originate from the classic work of Kiprianov and co-workers [12] and other publications [13,14]. Such publications reveal that the interaction between two uniform, partially conjugated chromophores results in the splitting of the long-wavelength absorption band of the parent "monomeric" dye into two bands. One of these new bands is red-shifted whilst the other is blue-shifted compared to the original long-wavelength band of the parent dye. The magnitude of the splitting depends on the symmetry of the interacting parent chromophores insofar as the higher the symmetry the more pronounced the splitting. The relative intensities of the split bands depend on the angle between the interacting chromophores: the larger the angle the greater is the intensity of the long-wavelength band and the lower the intensity of the short-wavelength band. When the angle is ~180°, only the long-wavelength band is observed. Thus, biscyanine dyes with bridged centrosymmetrical benzodioxazole **1** [15], benzodithiazole **2** [16], benzodiimidazole **3** [17], and benzodipyrrolenine **4a**, **5**, **6** [18] moieties (Scheme 1) have only one intense long-wavelength band. At the same time two bands appear in the absorption spectra of isomeric benzodipyrrolenine-based biscyanines **7** and **8** and these bands have lower intensity than those of the centrosymmetrical benzodipyrrolenine **4a** [18]. Despite the favourable absorption characteristics of **4a**, i.e.

---

* Corresponding author at: SSI "Institute for Single Crystals" of the National Academy of Sciences of Ukraine, 60 Lenin Ave., Kharkov 61001, Ukraine. Tel.: +38 057 3410272; fax: +38 057 3409343.
E-mail address: patsenker@isc.kharkov.com (L.D. Patsenker).

0143-7208/$ – see front matter © 2009 Elsevier Ltd. All rights reserved.
doi:10.1016/j.dyepig.2009.09.007

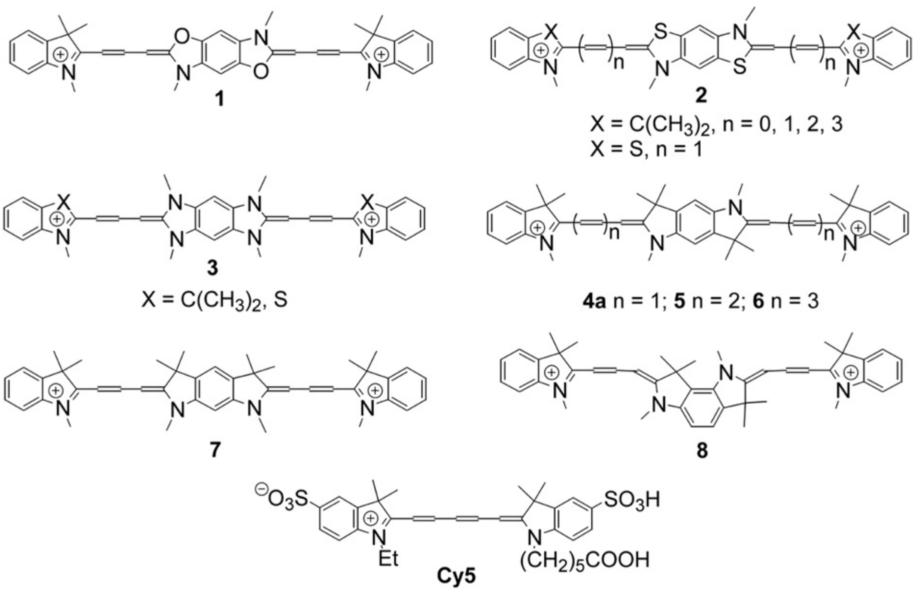

Scheme 1.

longer-wavelength absorption and higher extinction coefficient, the fluorescent properties of this dye have not been studied. Derivatized **4a** containing other terminal heterocyclic moieties such as benzoxazole, benzothiazole and quinoline have not been synthesized and investigated.

This work concerns the synthesis of a series of symmetrical biscyanine dyes based on centrosymmetrical benzodipyrrolenine and an investigation of the molecular structure, absorption and fluorescent properties of the dyes.

2. Experimental

2.1. General

Chemical reactions were monitored by TLC (Silica Gel 60 F_{254} TLC Plates, Merck). ^{1}H NMR spectra were measured on a *Varian Mercury-VX-200* (200 MHz) spectrometer in DMSO-d_6 using TMS as an internal standard.

Absorption spectra were taken at room temperature on a *Perkin-Elmer Lambda 35* UV/Vis spectrophotometer. Absorption maxima were obtained with an accuracy of 0.5 nm. For measurement of the extinction coefficients (ε), each dye (7–10 mg) was dissolved in 50 mL of methanol, the stock solution was diluted (1:2000) and the absorbance (*A*) was measured in a 5-cm standard quartz cell. The dye concentrations were in the range of $1.0–3.0 \times 10^{-7}$ M. The extinction coefficients were calculated according to the Lambert–Beer's law. The ε of each dye was independently measured several times and the average value was taken. The reproducibility for determining the extinction coefficients was about 1000 M^{-1} cm^{-1}.

Emission spectra and quantum yields were measured in chloroform and methanol at room temperature in a standard 1-cm quartz cell on a *Varian Cary Eclipse* spectrofluorometer. Concentrations were adjusted to be 1.0 to 3.0×10^{-7} M. The spectra were corrected. For the determination of the quantum yields, the integrated relative intensities of the dyes were measured against Cy5 in water as the reference. Optical density of the dye solutions at the excitation wavelength (610 nm) was between 0.12 and 0.18 measured in a 5-cm cell. The emission spectra of the solutions were recorded and the absolute quantum yields (φ) of the dyes were determined as described in [19] using Cy5 (Scheme 1, $\varphi = 27\%$) [20] as the reference dye. The quantum yields of each sample were independently measured 3–4 times and the average value was calculated. The reproducibility was no worse than 5%.

FAB-MS experiments were performed using magnetic sector mass spectrometer *MI-1201E* ("SELMI" Works, Sumy, Ukraine) equipped with commercial FAB units. Argon was used as a bombarding gas, the energy of the primary beam was 4.5 keV. All the compounds except **9** were injected using glycerol as the matrix while **9** was dissolved in 3-nitrobenzyl alcohol (NBA).

Quantum chemical semi-empirical simulations were done by the PM3 method using standard parameterization [21,22]. Full geometry optimization of the ground state was undertaken. PPP CI calculations [23,24] were carried out for the PM3 optimized geometries using the following parameters [25]: $\beta_{CN} = -1.9$ eV, $\beta_{CC} = -2.1$ eV, $E_N = -21.22$ eV, $\gamma_{NN} = 12.98$ eV.

Quinaldine and lepidine for synthesis were from Aldrich. Other chemicals, reagents and solvents were from Merck.

2.2. Synthesis

2.2.1. 1,3,3,5,7,7-Hexamethyl-2,6-dimethylene-1,2,3,5,6,7-hexahydropyrrolo[2,3-f]indole (10) [26]

Yield 98%; mp. 205–207 °C. ^{1}H NMR (200 MHz, DMSO-d_6, ppm): δ 6.62 (s, 2H), 3.72 (d, *J* = 3.3 Hz, 4H), 2.96 (s, 6H), 1.27 (s, 12H); Elemental analysis: calcd (%) for $C_{18}H_{24}N_2$: C, 80.55; H, 9.01; N, 10.44, found: C, 80.83; H, 9.10; N, 10.07.

2.2.2. 2-{6-(-1-Formylmethylidene)-1,3,3,5,7,7-hexamethyl-1,2,3,5,6,7-hexahydropyrrolo[2,3-f]indol-2-yliden}acetaldehyde (9)

$POCl_3$ (caution: corrosive; toxic; reacts violently with water; incompatible with many metals, alcohols, amines, phenol, DMSO, strong bases) (0.21 mL, 2.3 mmol) was added (with care) dropwise to dry DMF (2 mL) at 10 °C. The mixture was stirred for 1 h and dimethylene indole **10** (286 mg, 1 mmol) in dry DMF (2 mL) was added. The mixture was refluxed for 1 h, cooled, poured into solution of NaOH (2.5 g) in water (15 mL) and stirred for 30 min at room temperature. The precipitate was filtered, washed several times with water and air-dried to give the product as a yellow solid. Yield: 0.28 g (86%); mp. > 300 °C. ^{1}H NMR (200 MHz, DMSO-d_6, ppm): δ 9.84 (d, *J* = 8.8 Hz, 2H), 7.31 (s, 2H), 5.24 (d, *J* = 8.8 Hz, 2H), 3.26 (s, 6H), 1.61 (s, 12H); FAB-MS (NBA) m/z: 324 $(M)^+$, 325 $(MH)^+$; ν_{max} (KBr) 1604.8 cm^{-1} (C=O); Elemental analysis: calcd (%) for $C_{20}H_{24}N_2O_2$: C, 74.04; H, 7.46; N, 8.64, found: C, 73.87; H, 7.54; N, 8.50.

2.2.3. *General procedure to synthesize quaternary salts (**12a–12e**)*

Corresponding nitrogen containing heterocyclic compound (1 equivalent) was melted with methyl 4-methyl-1-benzenesulfonate (1.3 equivalents) at 130 °C for 3 h. The mixture was cooled to room temperature, treated with isopropanol, filtered and dried.

2.2.3.1. 1,2,3,3-Tetramethyl-3H-indolium 4-methyl-1-benzenesulfonate (12a). Yield 87%; ^{1}H NMR (200 MHz, DMSO-d_6, ppm): δ 7.94–7.86 (m, 1H), 7.84–7.78 (m, 1H), 7.66–7.57 (m, 2H), 7.46 (d, $J = 7.6$ Hz, 2H), 7.09 (d, $J = 7.6$ Hz, 2H), 3.96 (s, 3H), 2.75 (s, 3H), 2.28 (s, 3H), 1.5 (s, 6H); Elemental analysis: calcd (%) for $C_{19}H_{23}NO_3S$: C, 66.06; H, 6.71; N, 4.05; S, 9.28; found: C, 66.84; H, 6.64; N, 4.10; S, 8.81.

*2.2.3.2. 2,3-Dimethyl-1,3-benzoxazol-3-ium 4-methyl-1-benzenesulfonate (**12b**).* Yield 75%; ^{1}H NMR (200 MHz, DMSO-d_6, ppm): δ 7.48 (d, $J = 7.6$ Hz, 2H), 7.24–7.15 (m, 2H), 7.12 (d, $J = 7.6$ Hz, 2H), 6.95 (d, $J = 8.4$ Hz, 1H), 6.84 (t, $J = 7.4$ Hz, 1H), 3.01 (s, 3H), 2.28 (s, 3H), 1.68 (s, 3H); Elemental analysis: calcd (%) for $C_{16}H_{17}NO_4S$: C, 60.17; H, 5.37; N, 4.39; S, 10.04; found: C, 60.36; H, 5.34; N, 4.27; S, 9.92.

*2.2.3.3. 2,3-Dimethyl-1,3-benzothiazol-3-ium 4-methyl-1-benzenesulfonate (**12c**).* Yield 90%; ^{1}H NMR (200 MHz, DMSO-d_6, ppm): δ 8.42 (d, $J = 8.2$ Hz, 1H), 8.28 (d, $J = 8.2$ Hz, 1H), 7.95–7.74 (m, 2H), 7.46 (d, $J = 7.6$ Hz, 2H), 7.09 (d, $J = 7.6$ Hz, 2H), 4.19 (s, 3H), 3.16 (s, 3H), 2.28 (s, 3H); Elemental analysis: calcd (%) for $C_{16}H_{17}NO_3S_2$: C, 57.29; H, 5.11; N, 4.18; S, 19.12; found: C, 57.34; H, 5.22; N, 4.32; S 18.56.

*2.2.3.4. 1,2-Dimethylquinolinium 4-methyl-1-benzenesulfonate (**12d**).* Yield 84%; ^{1}H NMR (200 MHz, DMSO-d_6, ppm): δ 9.07 (d, $J = 8.4$ Hz, 1H), 8.56 (d, $J = 9.0$ Hz, 1H), 8.38 (d, 8.0 Hz, 1H), 8.21 (t, $J = 8.0$ Hz, 1H), 8.01 (d, $J = 8.7$ Hz, 1H), 7.97 (t, $J = 8.0$ Hz, 1H), 7.46 (d, $J = 7.6$ Hz, 2H), 7.09 (d, $J = 7.6$ Hz, 2H), 4.43 (s, 3H), 3.06 (s, 3H) 2.28 (s, 3H). Elemental analysis: calcd (%) for $C_{18}H_{19}NO_3S$: C, 65.63; H, 5.81; N, 4.25; S, 9.73; found: C, 65.54; H, 5.62, N 4.22; S, 10.12.

*2.2.3.5. 1,4-Dimethylquinolinium 4-methyl-1-benzenesulfonate (**12e**).* Yield 81%; ^{1}H NMR (200 MHz, DMSO-d_6, ppm): δ 9.34 (d, $J = 6$ Hz, 1H), 8.51 (t, $J = 9.6$ Hz, 2H), 8.27 (t, $J = 9.6$ Hz, 1H), 8.10–8.00 (m, 2H), 7.46 (d, $J = 7.6$ Hz, 2H), 7.09 (d, $J = 7.6$ Hz, 2H), 4.57 (s, 3H), 3.00 (s, 3H), 2.28 (s, 3H); Elemental analysis: calcd (%) for $C_{18}H_{19}NO_3S$: C, 65.63; H, 5.81; N, 4.25; S, 9.73; found: C, 65.50; H, 5.73; N, 4.20; S, 10.05.

2.2.4. *Dye **4a** (Method A)*

2-(1,1,3-trimethyl-2,3-dihydro-1*H*-2-indenyliden) acetaldehyde [27] (150 mg, 0.75 mmol) was dissolved in 5 mL acetic anhydride and then benzodipyrrolenine **11** (182 mg, 0.3 mmol) was added. The mixture was refluxed for 1 h, cooled and the product was precipitated with ether. The raw product was dissolved in a minimal amount of nitromethane and precipitated with ether to give the *title compound* ***4a*** (250 mg, yield of 85%).

2.2.5. *General procedure to synthesize dyes **4a–4e** (Method B)*

2-[1,3,3,5,7,7-hexamethyl-6-(2-oxoethylidene)-5,7-dihydropyrrolo[2,3-*f*]indol-2(1*H*,3*H*)-ylidene]acetaldehyde **9** (0.05 mmol) was dissolved in acetic anhydride (2 mL) and the corresponding nitrogen containing heterocyclic compound **12a–12e** (0.12 mmol) was added. The mixture was refluxed for 40 min and processed as described above to give the *title compound* **4a–4e.**

*2.2.5.1. Dye **4a**.* Yield 40 mg, 82%; mp. > 300 °C (dec). ^{1}H NMR (200 MHz, DMSO-d_6, ppm): δ 8.31 (t, $J = 13.4$ Hz, 2H), 7.85 (s, 2H), 7.65 (d, 2H), 7.53–7.39 (m, 8H), 7.38–7.25 (m, 2H), 7.11 (d, $J = 7.8$ Hz, 4H), 6.45 (d, $J = 13.4$ Hz, 4H), 3.69 (s, 6H), 3.65 (s, 6H), 2.28 (s, 6H), 1.73 (s, 12H) 1.7 (s, 12H); FAB-MS (Gl) m/z 621 $(Cat\text{-}CH_3)^+$, 635 $(Cat\text{-}H)^+$, 636 $(Cat^{++}+e^-)^+$, 807 $(Cat + An)^+$; Elemental analysis: calcd (%) for $C_{58}H_{66}N_4O_6S_2$: C, 71.13; H, 6.79; N, 5.72; S, 6.55; found: C, 71.33; H, 6.73; N, 5.69; S, 6.40.

*2.2.5.2. Dye **4b**.* Yield 23 mg, 50%; mp. > 300 °C (dec). ^{1}H NMR (200 MHz, DMSO-d_6, ppm): δ 8.29 (t, $J = 13.5$ Hz, 2H), 7.86 (d, $J = 7.0$ Hz, 2H), 7.77 (d, $J = 7.0$ Hz, 2H), 7.70 (s, 2H), 7.60–7.49 (m, 4H), 7.46 (d, $J = 7.6$ Hz, 4H), 7.10 (d, $J = 7.6$ Hz, 4H), 6.31 (d, $J = 13.5$ Hz, 2H), 6.20 (d, $J = 13.5$ Hz, 2H), 3.82 (s, 6H), 3.60 (s, 6H), 2.28 (s, 6H), 1.69 (s, 12H); FAB-MS (Gl) m/z 569 $(Cat\text{-}CH_3)^+$, 583 $(Cat\text{-}H)^+$, 584 $(Cat^{++}+e^-)^+$, 755 $(Cat + An)^+$; Elemental analysis: calcd (%) for $C_{52}H_{54}N_4O_8S_2$: C, 67.36; H, 5.87; N, 6.04; S, 6.92; found: C, 67.32; H, 5.94; N, 6.09, S 6.80.

*2.2.5.3. Dye **4c**.* Yield 32 mg, 68%; mp. > 300 °C (dec). ^{1}H NMR (200 MHz, DMSO-d_6, ppm): δ 8.08 (d, $J = 8.2$ Hz, 2H), 7.98 (t, $J = 13.5$ Hz, 2H), 7.87 (d, $J = 8.2$, 2H), 7.73 (s, 2H), 7.65 (t, $J = 8.2$, 2H), 7.51 (t, $J = 8.2$ Hz, 2H), 7.46 (d, $J = 7.6$ Hz, 4H), 7.09 (d, $J = 7.6$ Hz, 4H), 6.76 (d, $J = 13.5$ Hz, 2H), 6.25 (d, $J = 13.5$ Hz, 2H), 3.93 (s, 6H), 3.61 (s, 6H), 2.28 (s, 6H), 1.69 (s, 12H); FAB-MS (Gl) m/z 601 $(Cat\text{-}CH_3)^+$, 615 $(Cat\text{-}H)^+$; Elemental analysis: calcd (%) for $C_{52}H_{54}N_4O_6S_4$: C, 65.11; H, 5.67; N, 5.84; S, 13.37; found: C, 65.31; H, 5.71; N, 5.89; S, 13.04.

*2.2.5.4. Dye **4d**.* Yield 31 mg, 66.5%; mp. > 300 °C (dec). ^{1}H NMR (200 MHz, DMSO-d_6, ppm): δ 8.41–8.2 (m, 6H), 8.1 (d, $J = 8.7$ Hz, 2H), 8.03 (d, $J = 8.7$ Hz, 2H), 7.88 (t, $J = 7.8$ Hz, 2H), 7.67–7.55 (m, 4H), 7.48 (d, $J = 7.8$ Hz, 4H), 7.1 (d, $J = 7.8$ Hz, 2H), 6.72 (d, $J = 13.0$ Hz, 2H), 6.28 (d, $J = 13.0$ Hz, 2H), 4.11 (s, 6H), 3.58 (s, 6H), 2.28 (s, 6H), 1.73 (s, 12H); FAB-MS (Gl) m/z 589 $(Cat\text{-}CH_3)^+$, 603 $(Cat\text{-}H)^+$; Elemental analysis: calcd (%) for $C_{56}H_{58}N_4O_6S_2$: C, 71.01; H, 6.17; N, 5.91; S, 6.77; found: C, 71.21; H, 6.23; N, 5.86; S, 6.53.

*2.2.5.5. Dye **4e**.* After cooling, product was precipitated with ether and recrystallized from 2-propanol to give the *title compound* **4e** (yield 16 mg, 35%); mp. > 300 °C (dec). ^{1}H NMR (200 MHz, DMSO-d_6, ppm): δ 8.58 (d, $J = 8.5$ Hz, 2H), 8.52 (d, $J = 8.5$ Hz, 2H), 8.31 (t, $J = 13.4$ Hz, 2H), 8.13–7.96 (m, 6H), 7.78 (t, $J = 7.4$ Hz, 2H), 7.55 (s, 2H), 7.48 (d, $J = 7.8$ Hz, 4H), 7.25 (d, $J = 13.4$ Hz, 2H), 7.10 (d, $J = 7.8$ Hz, 4H), 6.24 (d, $J = 13.4$ Hz, 2H), 4.24 (s, 6H), 3.54 (s, 6H), 2.27 (s, 6H), 1.72 (s, 12H); FAB-MS (Gl) m/z 589 $(Cat\text{-}CH_3)^+$, 603 $(Cat\text{-}H)^+$, 604 $(Cat^{++}+e^-)^+$; Elemental analysis: calcd (%) for $C_{56}H_{58}N_4O_6S_2$: C, 71.01; H, 6.17; N, 5.91; S, 6.77; found: C, 71.10; H, 6.21; N, 6.08; S, 6.46.

3. Results and discussion

3.1. *Synthesis*

The key intermediate for the synthesis of biscyanines **4a–4e** is the quaternary salt **11** [26] that can be obtained by quaternization of 2,3,3,6,7,7-hexamethyl-3*H*,7*H*-benzo[1,2-*b*:3,4-*b*']dipyrrole (benzodipyrrolenine) with dimethylsulfate or methyltosylate. Biscyanine **4a** was reported to be synthesized with 42% yield by heating to reflux of the quaternized benzodipyrrolenine **11** with Fisher's aldehyde in acetic anhydride followed by removing of the solvent under the reduced pressure (Scheme 2, Method A) [18]. According to this procedure we synthesized compound **4** with a 62% yield. Furthermore instead of removing the solvent we precipitated the product with ether and after purification obtained **4a** in 85% yield.

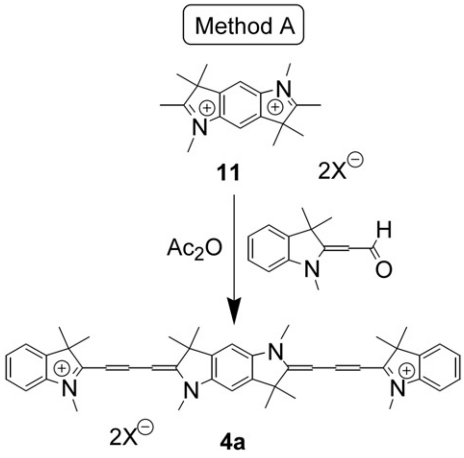

Scheme 2.

Nevertheless the above Method A seems not rational for synthesizing of biscyanines with variable terminal heterocyclic moieties because it requires prior formylation of each heterocyclic compound used as the terminal end-group (Scheme 3).

Therefore we explored another approach *via* the previously unknown benzodipyrrolenine diformyl derivative **9** (Scheme 4, Method B) [28]. Benzodipyrrolenine quaternary salt **11** cannot be formylated and therefore this salt was initially transformed into dimethylene benzodiindole **10** by treatment with aqueous ammonia. The Vilsmeier formylation of **10** with $POCl_3$ in an excess of DMF yielded the dialdehyde **9** in 86% yield.

Bis-trimethine dyes **4a–4e** were obtained with 35–82% yield by condensation of dialdehyde **9** with quaternized 2,3,3-trimethylindolenine **12a**, 2-methylbenzoxazole **12b**, 2-methylbenzothiazole **12c**, 2- and 4-methylquinolines (**12d** and **12e**), respectively (Scheme 4). Reactions were accomplished by refluxing in acetic anhydride. Structures of the synthesized dyes were confirmed with ^{1}H NMR (DMSO-d_6) and FAB-MS. Four doublet and two triplet signals of methine hydrogen atoms in the ^{1}H NMR spectra are located between 5.6 and 8.8 ppm.

The yield of dye **4a** synthesized according to Method B (Scheme 4) is 82%, which is substantially higher than that reported by Mihailenko et al. [18] (42%), and very close to the value of 85% that we obtained following the above improved Method A (Scheme 2). Thus the proposed approach to synthesize bis-trimethine dyes *via* diformyl derivative **9** seems to be good alternative for the previously described condensation of the Fisher's aldehyde with benzodipyrrolenine. The new approach is more convenient for the synthesis of a series of symmetrically substituted dyes with variable terminal end heterocyclic moieties.

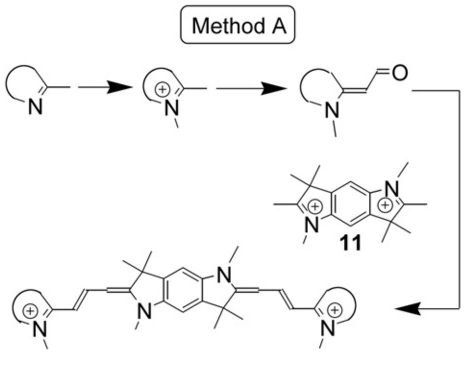

Scheme 3.

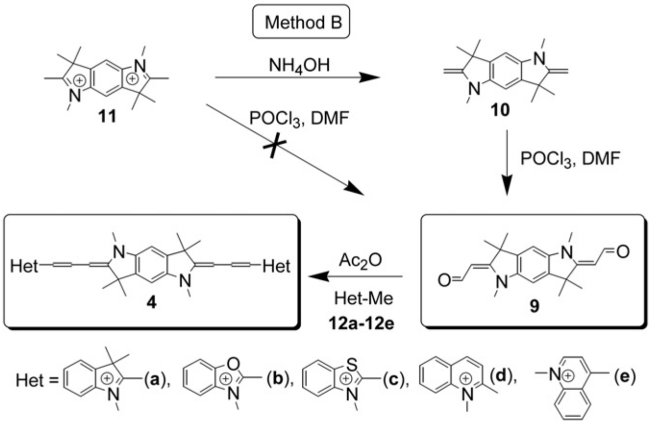

Scheme 4.

3.2. Molecular structure

The molecular structures of biscyanines **4a–4e** were studied using the PM3 semi-empirical quantum-chemical method. The simulations show that the dye molecules are flat, i.e. both terminal and central heterocycles are in plane. Quaternized nitrogen atoms of the central and terminal heterocycles (or quinoline benzene ring in case of **4e**) can be directed in one side (*syn*-form) or opposite sides (*anti*-form). Conformational analysis evidences that the *syn*-, *syn*-conformer (Fig. 1) is more preferable compared to both *anti*-, *anti*- and *syn*-,*anti*-forms by 4.2–11.3 kcal/mol and 1.7–7.4 kcal/mol, respectively (Table 1). Change of other torsion angles in the polymethine chain causes even more pronounced energy increase and therefore formation of the corresponding conformers is not very probable. According to the Boltzmann distribution the biscyanine molecules exist at room temperature mostly in the *syn, syn*-form. In this form the angle between two trimethine chromophore systems is very close to 180°.

The chromophore part of biscyanine molecules is presented as a di-cation with a delocalized positive charge. According to PM3 (Table 1) and PPP simulations the positive charge (q) predominates on the nitrogen atoms of the terminal heterocycles (q_{Term}) but also (to a lesser degree) on nitrogen atoms of the central benzodipyrrolenine moiety (q_{Centr}). Thus the electron

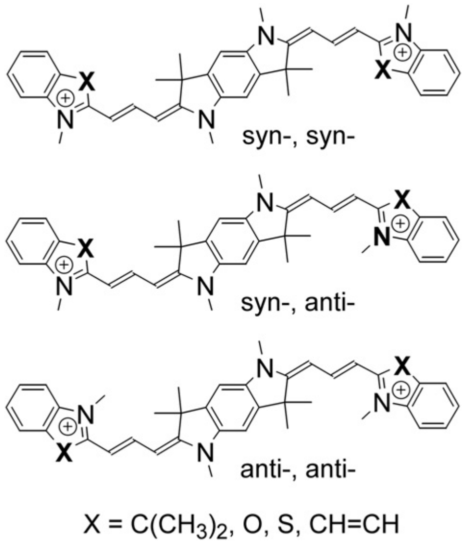

Fig. 1. Representative conformations of biscyanines **4a–4e**.

Table 1
The formation enthalpy (ΔH) of different conformers of biscyanines, the electron charges on nitrogen atoms of the central (q_{Centr}) and terminal (q_{Term}) heterocycles of the *syn,syn*-forms, and the chemical shifts of methyl hydrogen atoms of the central (δ_{Centr}) and terminal (δ_{Term}) heterocycles.

Molecule	$\Delta H_{\text{syn,syn}}$ [kcal/mol]	$\Delta H_{\text{syn,anti}}$ [kcal/mol]	$\Delta H_{\text{anti,anti}}$ [kcal/mol]	q_{Term}	q_{Centr}	δ_{Term} [ppm]	δ_{Centr} [ppm]	$\Delta\delta$ [ppm]
4a	414.7	418.8	422.9	+0.392	+0.226	3.69	3.65	0.04
4b	388.3	390.8	392.5	+0.303	+0.223	3.82	3.60	0.22
4c	469.3	471.7	474.5	+0.380	+0.228	3.93	3.61	0.32
4d	452.5	456.4	463.8	+0.414	+0.191	4.11	3.58	0.53
4e	453.2	456.8	460.7	+0.407	+0.178	4.24	3.54	0.70

density on the polymethine chains is shifted from the terminal heterocycles towards the central heterocyclic unit. The positive charge q_{Term} subsequently increases in the order of 2-benzoxazolium < 2-benzothiazolium < 2-indoleninium < 4-quinolinium < 2-quinolinium, while the positive charge q_{Centr} decreases in the order: 2-benzothiazolium > 2-indoleninium > 2-benzoxazolium > 2-quinolinium > 4-quinolinium, which does not correlate with the previous sequence. Because of the non-correlation between q_{Term} and q_{Centr} these electron charges cannot be used to make an unambiguous conclusion about the relative donating and withdrawing ability of the heterocyclic end-groups. It is worth mentioning that Brooker in his papers [29–31] investigated spectral shifts of the long-wavelength absorption band of heterocyclic compounds and concluded that the electron donor ability increases in the order of 2-indoleninium < 2-benzoxazolium < 2-benzothiazolium < 2-quinolinium < 4-quinolinium, which is different from our findings on the strength of the calculated electron charge distribution.

We found a clear correlation ($r = 0.95$) between the chemical shifts of the methyl hydrogens located on the nitrogen atoms of the terminal (δ_{Term}) and central (δ_{Centr}) heterocycles in the ^{1}H NMR spectra (DMSO-d_6) of biscyanines (Table 1). These shifts indicate that the electron donor ability of the terminal heterocycles increases in the order of 2-indoleninium < 2-benzoxazolium < 2-benzothiazolium < 2-quinolinium < 4-quinolinium. This sequence completely coincides with the Brooker's series obtained from the shifts of the absorption bands. Increasing difference between the chemical shifts $\Delta\delta = \delta_{\text{Term}} - \delta_{\text{Centr}}$ indicates that the electron asymmetry of polymethine chains increases in the order: **4a** < **4b** < **4c** < **4d** < **4e**.

The discussed spatial and electron structure of biscyanines have strong influence on their spectral properties.

3.3. Spectral properties

Absorption and emission spectra of biscyanines **4a–4e** were measured in chloroform and methanol. The spectral characteristics such as the absorption and emission maxima ($\lambda_{\max}$), extinction coefficients (ε), Stokes' shifts ($\Delta\nu_{\text{st}}$), quantum yields (Q.Y.), absorption and emission band half-widths ($\Delta\nu_{1/2}$) are given in Table 2. For a comparison the same table also includes the spectral characteristics of parent trimethine dyes **13–21** taken from [32,33]. Representative absorption and emission spectra of biscyanines in the example of **4a** are shown on Fig. 2.

Shape of Spectra. As predicted by Kiprianov's theory [12–14], due to the linear orientation of the two chromophores, all biscyanine dyes **4a–4e** show only one intensive long-wavelength absorption band in visible spectral range (Fig. 2). This band consists of two components: a longer-wavelength component with higher intensity and a shorter wavelength component with lower intensity. Similar to other cyanine dyes these components can be attributed to the vibrational transitions [34]. The shape of the absorption and emission spectra is found to be not dependent upon concentration in the range of $1.0–3.0 \times 10^{-7}$ M, which is evidence that the shorter wavelength component is not due to aggregation. The vibrational structure of the absorption band is more apparent in case of dye **4a** with the most symmetrical chromophore systems. An increase of the chromophores asymmetry, estimated by $\Delta\delta$ values (Table 1), and an increase of the solvent polarity cause a smoothing of the absorption and emission bands (Fig. 3). This effect originates from an increase of the dye molecule polarity and increase of interaction between the dye and solvent molecules [35,36]. At the same time no correlation between the $\Delta\delta$ values and the absorption and emission band half-widths ($\Delta\nu_{1/2}$) measured in chloroform and methanol (Table 2) was found.

Absorption and emission maxima of biscyanines are red-shifted by about 90–120 nm compared to those for the correspondent parent trimethines **13–21** (Table 2). To analyze correlation between spectral properties and molecular structure of both biscyanines and parent trimethines we simulated the spatial and electronic structure of these molecules in the ground and first excited states an calculated the electron transitions under excitation. The simulations were performed using semi-empirical quantum-chemical PM3 CI and PPP CI methods. An example of the calculated singlet electron transitions is shown on Fig. 2. These simulations evidence that the long-wavelength band of biscyanines is connected with $S_0 \rightarrow S_1^*$ transitions mostly formed by superposition of two configurations: HOMO → LUMO (higher contribution) and (HOMO − 1) → (LUMO + 1) (lower contribution). Calculated by PM3 CI method structures of the molecular orbitals participating in excitation $S_0 \rightarrow S_1^*$ (Fig. 4) and the localization numbers obtained by the PPP CI method (Fig. 5) indicate that the $S_0 \rightarrow S_1^*$ transition affects mostly two polymethine chains including nitrogen atoms of both central and terminal heterocyclic moieties. The angle between these two trimethine chromophore systems is very close to 180° and the electron transition is polarized along the principle axis of these chromophores.

The simulations indicate that the conjugation of two parent trimethines to form a biscyanine dye does not cause a noticeable change in the spatial and conformational structure of the parent chromophores. Localizations and polarizations of the $S_0 \rightarrow S_1^*$ transitions are also almost constant (Fig. 5). The nature of the heterocyclic end-groups does not noticeably impact the conformational structure of the molecules, the orientation of the two conjugated chromophores or the localization of the electron excitation but can substantially affect the transition energy and electron distribution in both ground and first excited states. The alteration of electron distribution upon the nature of the end heterocycles might lead to various positive and negative solvation effects for the investigated biscyanine dyes.

Indeed the location of the absorption and emission bands of biscyanines was experimentally found to be strongly dependent upon the structure of terminal heterocycles (Table 2). Thus a substitution of indolenine moiety with 2-quinoline results in the long-wavelength shift of the absorption (by 37 nm in chloroform and 22 nm in methanol) and emission maxima (63 and 61 nm). Introduction of 4-quinoline moiety causes even higher red-shifts. Substitution of an

Table 2
Spectral characteristics of biscyanines and parent trimethine dyes.

	Dye	Solvent	λ_{max} (Abs) [nm]	ε [M^{-1} cm^{-1}]	λ_{max} (Em) [nm]	$\Delta\nu_{st}$[a] [cm^{-1}]	Q.Y. [%]	$\Delta\nu_{1/2}$ (Abs)[b] [cm^{-1}]	$\Delta\nu_{1/2}$ (Em)[c] [cm^{-1}]
4a	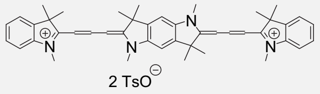	$CHCl_3$	658		677	430	18.8	1908	1835
		MeOH	644	251,000	664	470	10.4	1875	1930
4b	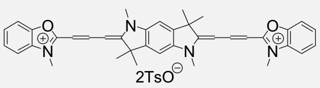	$CHCl_3$	616		640	610	28.3	2173	1812
		MeOH	596	154,000	629	880	12.6	2308	2180
4c	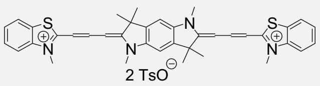	$CHCl_3$	664		688	525	23.0	1985	1000
		MeOH	640	205,200	675	810	6.0	2165	2200
4d	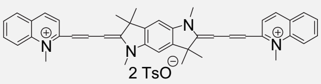	$CHCl_3$	695		740	875	4.0	2322	2400
		MeOH	666	176,000	725	1220	0.5	2230	2800
4e	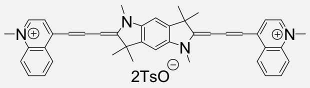	$CHCl_3$	707		755	900	3.8	2099	1420
		MeOH	717	133,700	773	1010	0.03	2209	1930
13	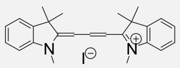	CH_2Cl_2	550	135,000	570	638	4	N/A	N/A
		EtOH	545	134,000	568	743	3		
14	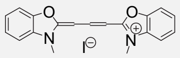	DMSO	490	N/A	515	991	9.3	N/A	N/A
		EtOH	482	156,000	500	747	4		
15	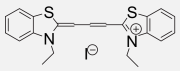	CH_2Cl_2	560	151,000	580	616	6	N/A	N/A
		EtOH	558	138,000	577	590	5		
16	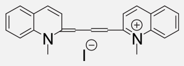	DMSO	615	N/A	645	756	0.4	N/A	N/A
		EtOH	605	178,500					
17	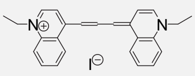	CH_2Cl_2	713	N/A	732	364	2	N/A	N/A
		DMSO	710	N/A	734	461	3.6		
18	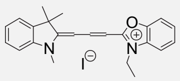	n-PrCN	512	N/A	534	805	4.6	N/A	N/A
		EtOH	510	112,700	n/d	n/d	n/d		
19	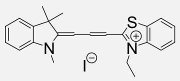	CH_2Cl_2	550	142,000	572	699	5	N/A	N/A
		EtOH	546	126,000	573	863	3		
20	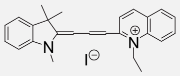	CH_2Cl_2	571	N/A	607	1039	0.7	N/A	N/A
		EtOH	561	106,900	622	1748	0.3		
21	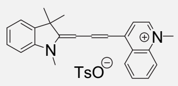	CH_2Cl_2	618	N/A	644	653	1.6	N/A	N/A
		EtOH	601	79,800	653	1324	0.7		

[a] $\Delta\nu_{st}$ — Stokes' shift.
[b] $\Delta\nu_{1/2}$ (Abs) — Absorption band half-width.
[c] $\Delta\nu_{1/2}$(Em) — Emission band half-width.

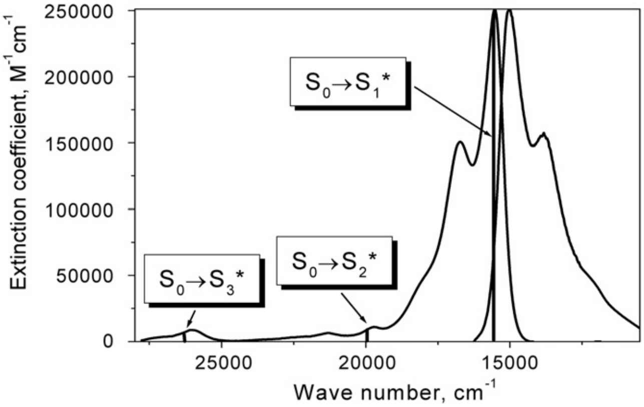

Fig. 2. Absorption and emission spectra of biscyanine **4a** in methanol and electron transitions calculated by PPP CI method.

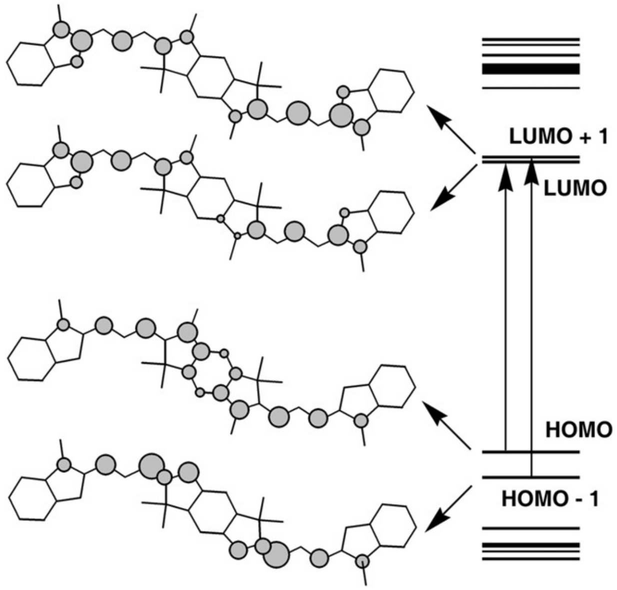

Fig. 4. Structure of the boundary orbitals in molecule **4b** obtained by PM3 CI method.

indolenine with a 2-benzothiazole does not result in a sensible change of absorption wavelength (red-shift by 6 nm in chloroform and blue-shift by 4 nm in methanol) but the fluorescence maximum is red-shifted by 11 nm in both solvents. The absorption and emission maxima of the benzoxazole derivative **4b** are blue-shifted as compared to the indolenine-based dye **4a**. We found clear correlations between the absorption and emission maxima measured in both chloroform and methanol (Table 2) and $\Delta\delta$ values (Table 1). The correlation coefficients (r) are in the range of 0.77–0.88 depending on the solvent system. Only indolenine-based dye **4a**, which has longer absorption and emission maxima as compared to benzoxazole derivative **4b**, demonstrates a pronounced deviation from the regression. Elimination of **4b** from the regressions results in noticeable increase of the correlation coefficients ($r = 0.94$–0.99). Similar correlations were found for parent trimethines **13–21**, where benzoxazole derivatives were also dropped out of the regressions.

The spectral characteristics of biscyanines are noticeably dependent upon the solvent system (Table 2). All dyes except **4e** exhibit a hypsochromic blue-shift of the absorption maxima when chloroform is replaced with methanol. The most pronounced blue-shift of 29 nm is found for **4d**. The emission maxima in methanol are also blue-shifted compared to those in chloroform but this effect is less pronounced for the emission maxima as compared to the absorption maxima, which probably is the result of the lower polarity these dye molecules have in the excited state. Thus the calculated by the PM3 method dipole moment of **4a** is 0.23 D in the ground state and 0.17 D in the first excited state. Dye **4e** exhibits red-shifted absorption (10 nm) and emission (18 nm) maxima when chloroform is substituted with methanol. An increase in solvent polarity causes an increase of the Stoke's shifts and decrease of the quantum yields, which is most likely the result of an increase in internal conversion caused by interaction between the solvent of higher polarity and the polar dye molecules in the excited state.

Similar to the parent trimethine dyes **13–21** [37,38] the above spectral shifts caused by solvent polarity and the heterocyclic end-groups in biscyanine dyes **4a–4e** can be understood by considering the donor-acceptor abilities of these heterocycles. The heterocyclic end-groups in trimethine dyes **13–21** and biscyanine dyes **4a–4e** substantially differ in their electron donating and electron withdrawing properties. The different electronic effects caused by the heterocyclic end-groups in the parent trimethine dyes **13–21** are known to cause an imbalance in the molecules electronic symmetry in the ground state but in the excited state the electron

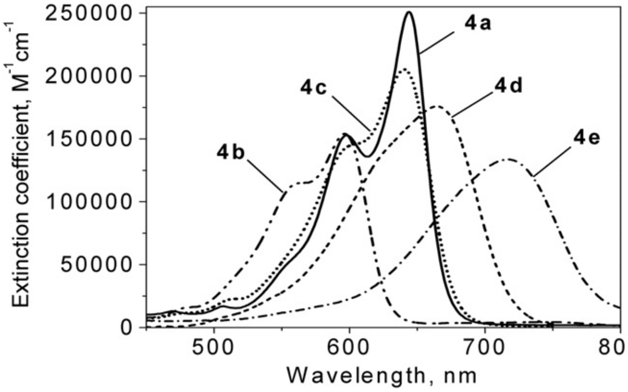

Fig. 3. Influence of terminal heterocycles on the long-wavelength absorption bands of biscyanine dyes **4a–4e** in methanol.

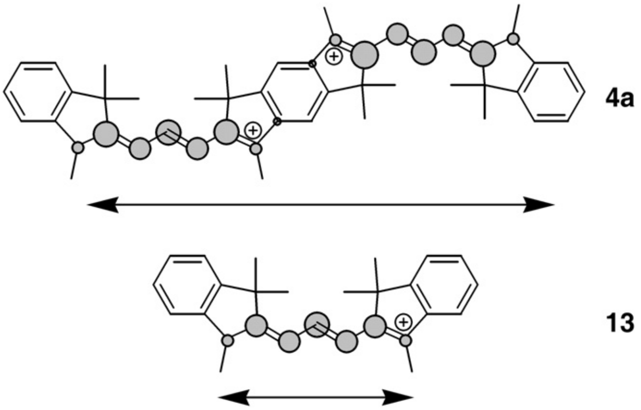

Fig. 5. Localization and polarization of electron transition $S_0 \rightarrow S_1^*$ in biscyanine **4a** and parent trimethine **13** molecules (PPP CI method).

density evens out substantially: the more the heterocycles end-groups differ from each other the stronger the electron charge redistribution under excitation [36]. The charge redistribution in the excited state initiates intramolecular (conformational) and intermolecular (between dye and solvent molecules) relaxation which results in the Stokes' shift increase due to the increase of both the molecular asymmetry and the solvent polarity [37]. In addition because the unsymmetrical trimethine dyes **18–21** have substantially higher polarity in the ground state compared to the excited state, their absorption spectra are more sensitive towards the solvent polarity than the emission spectra.

Similar effects are observed for biscyanine dyes **4a–4e**. Despite the biscyanine molecules are symmetric they consist of two uniformly unsymmetrical trimethine chromophores. In order to quantify this asymmetry we used the chemical shifts ($\Delta\delta$) observed for the methyl hydrogens that are located on the nitrogen atoms of terminal and central heterocycles (Table 1). $\Delta\delta$ shows a minimal value in **4a** indicating the highest chromophore symmetry as compared to other biscyanines. As a result the Stokes' shift ($\Delta\nu_{st}$) for **4a** has also the minimal value of 430 cm^{-1} in chloroform and 470 cm^{-1} in methanol (Table 2). Biscyanines **4b** and **4c** containing stronger electron-donor benzoxazole and benzothiazole groups have bigger $\Delta\delta$ and therefore larger Stokes' shifts of 610 and 525 cm^{-1} in chloroform and 880 and 810 cm^{-1} in methanol, respectively. A further increase in the electron-donor ability of the heterocyclic end-groups in 2- and 4-quinolinium derivatives **4d** and **4e** causes an even more pronounced increase of $\Delta\delta$ and $\Delta\nu_{st}$. We found clear correlation ($r = 0.93$ in chloroform and of $r = 0.86$ in methanol) between $\Delta\delta$ and $\Delta\nu_{st}$.

Data in Table 2 demonstrate that in general biscyanine dyes **4a–4e** have higher **extinction coefficients and quantum yields** than the parent symmetrical trimethines **13–17** and especially the unsymmetrical parent dyes **18–21**. The quantum yields decrease when chloroform is substituted with methanol. This effect is well-known to be explained by quenching of polar dye molecules in polar solvents.

The absorption and emission maxima and quantum yields of biscyanine dyes were found to correlate well with those values of parent trimethine dyes ($r = 0.94$–0.99). These correlations evidence that the combination of two trimethine chromophores into one biscyanine molecule yields compounds with similar solvation effects, and similar influence of the heterocyclic end-groups on the spectral properties.

4. Conclusions

The condensation of benzodipyrrolenine diformyl derivative with quaternized heterocyclic CH-acidic compounds is a convenient way to synthesize bis-trimethine dyes with variable heterocyclic end-groups. Using this method a systematic series of biscyanines with different heterocyclic terminal moieties was synthesized and their spectral and luminescent properties were investigated. The fusion of two trimethine chromophores into one molecule leads to a substantial red-shift of the absorption and emission bands and an increase of the extinction coefficients and quantum yields. The influence of the heterocyclic end-groups on the spectral properties of biscyanines is similar to that in the series of their parent trimethine dyes. Substitution of both terminal benzoxazole moieties with indolenine, benzothiazole, 2- and 4-quinoline causes a consecutive red-shift of the absorption and emission maxima and a decrease of the quantum yields. A clear correlation was established between the electron asymmetry of the parent polymethine chains with the chemical shifts of the methyl hydrogens on the heterocyclic nitrogens.

Acknowledgement

This work was supported by the National Academy of Sciences of Ukraine, project No. 0107U000487.

References

[1] Hossain MZ, Ernst LA, Nagy JL. Utility of intensely fluorescent cyanine dyes (CY3) for assay of gap junctional communication by dye-transfer. Neurosci Lett 1995;184(1):71–4.
[2] Lewis JS, Achilefu S, Garbow JR, Laforest R, Welch MJ. Small animal imaging: current technology and perspectives for oncological imaging. Eur J Cancer 2002;38(16):2173–88.
[3] Weissleder R, Ntziachristos V. Shedding light onto live molecular targets. Nat Med 2003;9(1):123–8.
[4] Haugland R. Handbook of fluorescent probes and research products. 9th ed. USA: Mo-lecular Probes; 2002.
[5] Berneth Horst, Bruder Friedrich-Karl. Optical data carrier comprising a cyanine dye as light-absorbent compound in the information layer. US 2005042407 (B2); 2005.
[6] Metz Hans-Joachim, Mura Jean-Luc. Lightfast cyanine dye compositions for optical data recording. WO2005023939; 2005.
[7] Wurthner F, Wortmann R, Matschiner R, Lukaszuk K, Meerholz K, Denardin Y, et al. Merocyanine dyes in the cyanine limit: a new class of chromophores for photorefractive materials. Angew Chem Int Ed 1997;36(24):2765–8.
[8] West W, Gilman PB. In: James TJ, editor. The theory of the photographic process. New York: Macmillian; 1977.
[9] Araki T, Ito E, Oichi K, Mitsumoto R, Sei M, Oji H, et al. NEXAFS Spectroscopic study of organic photographic dyes and their adsorbed states on AgCl and AgBr. J Phys Chem B 1997;101(49):10378–85.
[10] Sibbett W, Taylor JR. Passive mode locking in the near infrared. IEEE J Quantum Electr 1984;20(2):108–10.
[11] Schäfer FP. Dye lasers. 3rd ed. Berlin: Springer-Verlag; 1990.
[12] Kiprianov AI. Absorption spectra of organic dyes containing two chromophores. Russ Chem Rev 1971;40(7):594–607.
[13] Borisevich YuE, Kuz'min VA, Renge IV. Effect of π-electron conjugation of the chromophores on the reactivity of the triplet states of dyes with two chromophores in electron-transfer reactions. Russ Chem Bull 1981;30(8):1465–70.
[14] Ibrayev NK, Ishchenko AA, Karamysheva RK, Mushkalo IL. Influence of interaction of chromophores, linked by the unconjugated chain, on the luminescence properties of biscyanine dyes. J Luminescence 2000;90(3):81–8.
[15] Mihailenko FA, Boguslavskaya AN. Cyanine dyes with two conjugated chromophores. X. Ukr Khim Zhurn 1969;35(9):943 [in Russian].
[16] Kiprianov AI, Mushkalo IL, Mihailenko FA. Cyanine dyes with two conjugated chromophores. IV. Zh Org Khim 1967;3(11):2041–7 [In Russian].
[17] Kiprianov AI, Fridman SG. Cyanine dyes with two conjugated chromophores. VI. Zh Org Khim 1968;4(4):696–703 [In Russian].
[18] Mihailenko FA, Boguslavskaya AN, Kiprianov AI. Biscyanines from isomeric benzodipyrrolenines. Chem Heter Comp 1971;7(5):578–80.
[19] Parker CA. Photoluminescence of solutions. Amsterdam: Elsevier; 1968.
[20] Mujumdar RB, Ernst LA, Mujumdar SR, Lewis CJ, Waggoner AS. Cyanine dye labeling reagents: sulfoindocyanine succinimidyl esters. Bioconjug Chem 1993;4(2):105–11.
[21] Stewart JJP. Optimization of parameters for semiempirical methods I. Method J Comput Chem 1989;10(2):209–20.
[22] Stewart JJP. Optimization of parameters for semiempirical methods II. applications. J Comput Chem 1989;10(2):221–32.
[23] Pariser R, Parr RG. A semi-empirical theory of the electronic spectra and electronic structure of complex unsaturated molecules. J Chem Phys 1953;21(3):466–71.
[24] Pople GA. Electron interaction in unsaturated hydrocarbons. Trans Faraday Soc 1953;49(12):1375–85.
[25] Fabian J, Zahradnic R. PPP-Berechnung zum vinylenschift symmetrischer farbstoff. Wiss Z Thechn Univ (Dresden) 1977;26(2):315–23.
[26] Mihailenko FA, Boguslavskaya AN. Synthesis of isomeric benzodipyrrolenines and their derivatives. Chem Heter Comp 1971;7(5):574–7.
[27] Fri H. Über α,β-ungesättigte β-Anilino-carbonyl-Verbindungen als Modellsubstanzen für den Chromophor von C-Curarin-III (C-Fluorocurarin). Chem Ber 1959;92(8):1809–17.
[28] Patent Application US 2007/0281363 A1.
[29] Brooker LG. Absorption and resonance in dyes. Rev Mod Phys 1942;14(2):275–93.
[30] Brooker LG, Sklar AI, Gressman HW, Keyes GH, Smith LA, Sprague RH, et al. Color and constitution. VII.[1] Interpretation of absorptions of dyes containing heterocyclic nuclei of different basicities. J Am Chem Soc 1945;67(11):1875–89.
[31] Brooker LG, Keyes GH, Sprague RH, Van Dyke RH, Van Lare E, Van Zandt G, et al. Color and constitution. X.[1] absorption of the merocyanines[2]. J Am Chem Soc 1951;73(11):5332–50.
[32] Ishchenko AA. Structure and spectral-luminescent properties of polymethine dyes. Kiev Naukova Dumka 1994 [in Russian].

[33] Richard CB, Henry AK. Absorption and fluorescence properties of cyanine dyes. J Chem Eng Data 1977;22(4):69–75.

[34] Permogorov VI, Dyadyusha GG, Mihailenko FA, Kiprianov AI. Electronic spectra of biscyanine dyes. Doklady AN SSSR 1969;188(5):1098–101 [in Russian].

[35] Ishchenko AA, Derevyanko NA, Kudinova MA, Dyadyusha GG, Tolmachev AI. Chemical structure and shape of the absorption bands of pyrylocyanine dyes. Theoret Exper Chem 1978;13(6):628–31.

[36] Ishchenko AA, Zubarovskii VM, Gromova GA, Derevyanko NA. Influence of polymetine chain length on absorption spectra of unsymmetric cyanine dyes. Zh Org Khim 1987;23(3):628–30 [in Russian].

[37] Kiprianov AI. Colour and structure of organic dyes. Ukr Khim Zhurn 1967;33(11):1169 [in Russian].

[38] Ishchenko AA, Derevyanko NA, Svidro VA. Constitution and fluorescence spectra of an-symmetryc polymethine dye. Dyes Pigments 1992;19(3):169–77.